Charge Transfer Dynamics in Polymer–Fullerene Blends for Efficient Solar Cells

ARTICLE *in* THE JOURNAL OF PHYSICAL CHEMISTRY B · DECEMBER 2009

Impact Factor: 3.3 · DOI: 10.1021/jp907840z · Source: PubMed

Charge Transfer Dynamics in Polymer−Fullerene Blends for Efficient Solar Cells

Dorota Jarzab,*,† Fabrizio Cordella,† Martijn Lenes,† Floris B. Kooistra,† Paul W. M. Blom,†,‡ Jan C. Hummelen,† and Maria A. Loi*,†

Zernike Institute for Advanced Materials, University of Groningen, Nijenborgh 4, 9747 AG Groningen, The Netherlands, and Holst Centre, High Tech Campus 31, 5605 KN Eindhoven, The Netherlands

Received: August 13, 2009; Revised Manuscript Received: November 5, 2009

Blends of poly(3-hexylthiophene) (P3HT) and the bis-adduct of [6,6]-phenyl-C_{61}-butyric acid methyl ester (bisPCBM) show enhanced performances in bulk-heterojunction solar cells compared to P3HT:PCBM thin films due to their higher open-circuit voltage. However, it is not clear whether the decrease of the short-circuit current observed in P3HT−bisPCBM blends originates from the 100 mV reduction of the offset between the lowest unoccupied molecular orbitals of the donor and the acceptor or from a change in the morphology. The analysis of the photoluminescence dynamics of the various bulk heterojunctions provides information on the dependence of the electron transfer process on their microstructure. We find that in solution, where the donor−acceptor distribution is homogeneous, the photoluminescence dynamics is the same for the bis- and PCBM-based blends, while in thin films the first shows a slower dynamics than the second. This result indicates that the reduction of the LUMO offset of ∼100 meV does not influence the electron transfer efficiency but that the diversity between the photoluminescence dynamics in thin films should be ascribed to the different microstructure of the bulk heterojunctions fabricated with the two acceptors.

1. Introduction

Fifteen years of research on organic solar cells has shown that the best performing devices have a so-called bulk heterojunction as the active layer.[1,2] The bulk heterojunction is a three-dimensional heterostructure composed of two materials: one of them is a light absorbing, electron-donating, and hole conducting polymer, and the other is an electron acceptor and electron-conducting fullerene derivative. The operating principle of this kind of solar cells can be described as a four-step process. In the first step, excitons are generated under illumination, which subsequently diffuse toward the organic−organic interface. At the interface the bound electron−hole pairs dissociate due to the high electron affinity of the fullerene derivative. Finally, the newly generated charge carriers are transported toward the respective electrodes.[3]

Due to the nature of their active layer, the performance of these devices not only depends on the material properties but also on the processing conditions.[4,5] These conditions determine the morphology and the microscopic structure of the blend, i.e., the size of the single-phase domains and of the interface. The strongest requirements on the active layer structure result from the exciton diffusion length in the polymer and the percolation pathway for the carriers. Since the electron transfer only occurs at the donor/acceptor interfaces, the ideal size of the polymer domains is determined by the exciton diffusion length. The typical diffusion length in conjugated polymers is ∼5−7 nm,[6,7] and therefore photogenerated excitons created farther from the interface than this length will recombine before being separated in charge carriers. On the other hand, the transport of the charge carriers toward to the respective electrodes requires the presence of a percolating pathway of neat polymer phase for the holes and of the fullerene phase for the electrons.

Several strategies have been put forward to increase the power conversion efficiency of these potentially low cost solar cells. These strategies are mainly dealing with the material properties, in particular: (i) a more favorable overlap of the absorption spectrum of the active layer with the solar emission,[8] (ii) a better charge carrier mobility,[9] and (iii) an optimized relative position of the energy levels of the donor and acceptor.[10] The last point is connected to the fact that the open circuit voltage V_{oc} in organic solar cells is limited by the energy difference between the highest occupied molecular orbital (HOMO) of the donor and the lowest unoccupied molecular orbital (LUMO) of the acceptor.[11] Calculations and experiments show that a rising of the LUMO level of the acceptor can lead to an enhancement of the efficiency of these photovoltaic devices.[11,12] On the other hand, it is also known that a certain minimum energy offset between the LUMO levels of the donor and the acceptor is necessary for the electron transfer to occur. Excessive lifting of the LUMO of the acceptor will therefore limit or even suppress the electron transfer process.

The most studied organic solar cells until now use as the active layer the blend of poly(3-hexylthiophene) P3HT and of the fullerene derivatives [6,6]-phenyl-C_{61}-butyric acid methyl ester (PCBM).[13] In this case, the difference between the LUMOs is about 1.1 eV[11] which by far exceeds the 0.3−0.5 eV that is considered to be sufficient for efficient charge separation.[14] Recently, Lenes et al.[10] have reported solar cells where a reduced offset between the donor and the acceptor LUMOs leads to an increase of the photovoltaic efficiency. The strategy of the authors was to use P3HT as a donor and the bis-adduct of PCBM (bisPCBM) as the acceptor, and the last has a LUMO level that is ∼100 meV higher than the one of the monoadduct acceptor molecule. The P3HT:bisPCBM solar cells fabricated with the slow drying technique showed a V_{oc} of 0.73 V, which is considerably higher than the V_{oc} reported for standard P3HT:PCBM-based devices (0.58 V). In spite of a slightly reduced short-circuit density (J_{sc}) from 104 to 96 A/m^2, the power

* To whom correspondence should be addressed. E-mail: d.m.jarzab@rug.nl; m.a.loi@rug.nl.
† University of Groningen.
‡ Holst Centre.

10.1021/jp907840z
Published on Web 12/08/2009

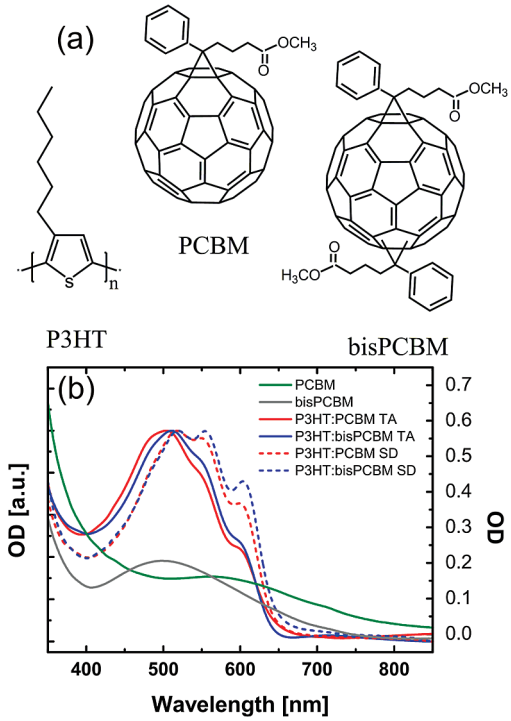

Figure 1. (a) Chemical structure of P3HT, PCBM, and bisPCBM and (b) optical density of PCBM (green curve) and bisPCBM (gray curve) thin films. Normalized optical density of P3HT:PCBM (red curve) and P3HT:bisPCBM (blue curve) thin films prepared by thermal annealing (TA, solid line) and by slow drying (SD, dashed line).

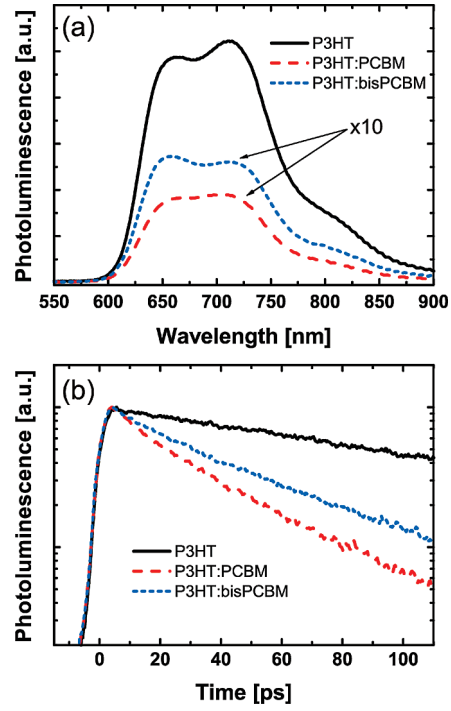

Figure 2. (a) Photoluminescence spectra and (b) dynamics detected at ~665 nm of P3HT, P3HT:PCBM, and P3HT:bisPCBM of thermal annealed films.

conversion efficiency of the bisPCBM-based devices was strongly enhanced from ~3.8% (P3HT:PCBM) to ~4.5% for slowly dried films. A similar trend is also shown by the devices prepared by the thermal annealing, with a power conversion efficiency of ~3% for P3HT:PCBM and ~3.6% for P3HT:bisPCBM. To further clarify the origin of the reduced J_{sc} and the operation of P3HT:bisPCBM devices, we investigate the photophysical properties of the bisPCBM- and PCBM-based blends. Time-resolved photoluminescence (PL) is a powerful tool for studying the charge transfer process in bulk heterojunctions.[15] Additionally, due to the fact that the dynamics of the PL is also monitoring the exciton diffusion, it can also provide information on the microstructure of the bulk heterojunction. To be able to unravel the effects of energy level variations and the microstructure of the bulk heterojunction structure, we study the PL dynamics of both PCBM- and bisPCBM-based blends in solution as well as in thin films prepared with different protocols, namely, spin coating followed by either thermal or solvent annealing (slow drying). In solution, the polymer and the fullerene derivatives are homogeneously distributed in the solvent, and the two blends show the same dynamics of the photoluminescence. Conversely, films of the P3HT:bisPCBM blend prepared by thermal annealing and slow drying show slower dynamics than the corresponding P3HT:PCBM films. These slower dynamics are determined by the fact that less excitons reach the donor−acceptor interface due to the nonoptimal three-dimensional structure of the bisPCBM-based bulk heterojunction. These findings demonstrate that the performance of P3HT:bisPCBM solar cells can be further increased by improvement of the bulk hererojunction microscopic structure.

2. Results

Figure 1(a) displays the chemical structure of P3HT and of the two fullerene derivatives PCBM and bisPCBM. P3HT is chosen for photovoltaic applications mainly due to the good overlap of its absorption spectrum with the solar emission and because of its high hole mobility (up to 5×10^{-3} cm^2 V^{-1} s^{-1} in solar cells).[16] PCBM is the most used electron acceptor in plastic solar cells, with its high electron affinity and an electron mobility of 2×10^{-3} cm^2 V^{-1} s^{-1}.[17] Both P3HT and the fullerene derivative show the tendency to crystallize, meaning that the morphology of the blend can be controlled by varying the processing conditions. In particular, thermal and solvent annealing have demonstrated to promote microsize crystallization.[6,18]

Figure 1(b) shows the absorption spectra of thin films of PCBM, bisPCBM, and of the bulk heterojunctions prepared by thermal annealing and slow drying. The absorption spectra for P3HT:PCBM films prepared by both techniques correspond to that reported by other authors.[13] Samples prepared by slow drying techniques show stronger absorption in the red region and more pronounced vibronic progression than films prepared by thermal annealing. The better resolved structure of the absorption spectra indicates the higher molecular organization of the slow dried films.[19] Both sets of samples do not present significant differences in the absorption spectra between P3HT:PCBM and P3HT:bisPCBM.

Figure 2(a) shows the PL spectra of P3HT, P3HT:PCBM, and P3HT:bisPCBM thin films, prepared by thermal annealing. The spectra show similar features, with two vibronic peaks centered at ~660 and ~710 nm and a shoulder at ~810 nm. There are no significant spectral differences between the neat polymer and the two blends. As expected, the blending of P3HT with fullerene derivatives gives rise to quenching of the PL intensity, being the first indication of electron transfer. In the case of P3HT:PCBM, the quenching is over 28 times and for P3HT:bisPCBM over 19 times (calculated integrating the whole spectra). This points to a more efficient charge transfer and exciton dissociation when PCBM is used as the acceptor. However, steady state photoluminescence is not the best tool

TABLE 1: PL Decays Fitting Parameters[a]

	A_1	τ_1 [ps]	A_2	τ_2 [ps]
P3HT thermally annealed	0.24	79	0.85	366
P3HT:PCBM thermally annealed	0.62	8	0.72	41
P3HT:bisPCBM thermally annealed	0.62	8	0.70	60
P3HT slowly dried	0.50	40	0.64	173
P3HT:PCBM slowly dried	0.50	8	0.76	31
P3HT:bisPCBM slowly dried	0.50	8	0.79	38
P3HT in solution 10 mg/mL (TR4)	0.12	170	0.91	510
P3HT:PCBM in solution 10 mg/mL (TR4)	0.17	52	0.95	413
P3HT:bisPCBM in solution 10 mg/mL (TR4)	0.17	52	0.95	413

[a] All decays were fitted with the function: $I_{PL}(t) = A_1 \cdot \exp(-t/\tau_1) + A_2 \cdot \exp(-t/\tau_2)$, where A_1, A_2 and τ_1, τ_2 are fitting parameters.

to study the electron transfer due to the fast dynamics of the process. Figure 2(b) shows the PL dynamics of the thermally annealed thin films of pristine P3HT, P3HT:PCBM, and P3HT:bisPCBM blends, detected at the 0−0 transition (~660 nm). The PL time dependence shows a biexponential decay for all the samples, with the first time constant significantly faster than the second. The PL decay of the neat P3HT thin film was fitted with time constants τ_1 ~79 ps and τ_2 ~366 ps. For the blends, a reduction of both lifetimes is observed. At short delays after the photoexcitation, the PL of the two blends can be fitted with τ_1 ~8 ps, whereas the second component has a lifetime τ_2 ~41 ps for P3HT:PCBM and τ_2 ~60 ps for P3HT:bisPCBM (see Table 1). The reduction of the PL decay time occurs in the same ratio for the fast (79 ps→8 ps) and slow (366 ps → 41 ps) components in the case of the PCBM-based blend. However, in the case of bisPCBM, the two time constants have a dissimilar behavior with τ_2 being more persistent. Since the lifetime of the PL in the blend results from the combination of exciton diffusion followed by an electron transfer process, the longer lifetime can be an indication for a larger size of the polymer domains. This would also be consistent with the lower J_{sc} as observed in the bisPCBM:P3HT blends.

To get insight into the working mechanism of the best performing devices, we carried out time-resolved PL measurement on the active layers of the devices fabricated as reported by Lenes et al.[10] The active layer was prepared with the slow drying technique that involves a solvent annealing process.[13] With such a technique, the device fabricated using P3HT:PCBM showed an efficiency of 3.8%, while for the P3HT:bisPCBM device it was increased up to 4.5%.[10] The steady state PL spectra of the active layer of these devices are reported in Figure 3(a). The PL spectra are blue-shifted with respect to the thermally annealed films (Figure 2) and have a more defined vibronic structure with peaks centered at ~640 and ~690 nm and a weak shoulder at ~790 nm. These spectra show a redistribution of the intensity between the vibronic features with respect to the spectra of the thermal annealed films. The more defined vibronic features indicate a better ordering of the polymer chains in the slowly dried films.[20,21] In the slow drying process, the solvent evaporation is less rapid than in the thermal annealing, allowing an increased reorganization of the molecules that results in a higher supramolecular order. The blue-shift of the PL shown by the slowly dried films compared to the thermally annealed ones indicates the suppression of the exciton migration toward the lower energy sites of the density of states of the polymer due to the electron transfer at shorter delays after the photoexcitation.[7] The earlier electron transfer is also reflected in the reduction of the PL intensity of the slowly dried films. Also in this case, the PL quenching is higher for the P3HT:PCBM blend

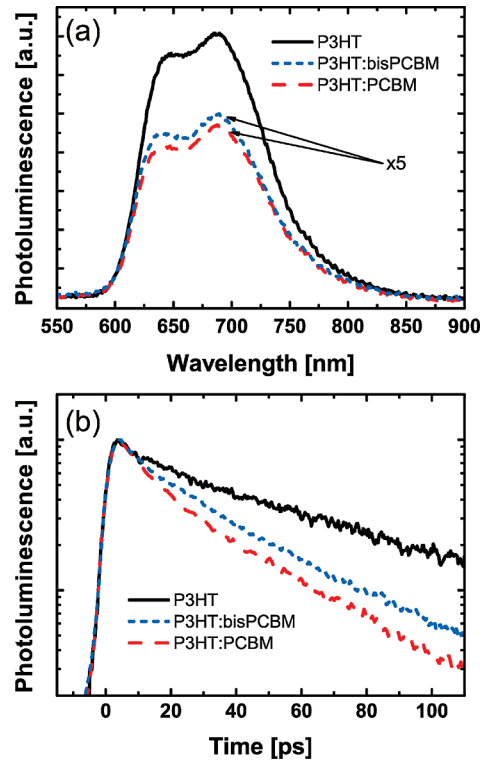

Figure 3. (a) Photoluminescence spectra and (b) dynamics detected at ~640 nm of P3HT, P3HT:PCBM, and P3HT:bisPCBM of slowly dried films.

(7.1 times) than for the P3HT:bisPCBM (6.6 times) one, but the difference between the quenching is strongly reduced as compared to the thermally annealed films. Also, the slowly dried thin films display a biexponential PL decay time. The PL decay of the pristine P3HT thin film was fitted with time constants τ_1 ~40 and τ_2 ~173 ps, which are substantially shorter than for the thermally annealed film. This effect could be ascribed to the better supramolecular order of the slowly dried samples and the higher delocalization of the excitons. In both blends, the fast component of the lifetime amounts to τ_1 ~8 ps with the same amplitude, similarly to the thermally annealed films. The slow component on the other hand has a lifetime τ_2 ~31 ps for P3HT:PCBM and τ_2 ~38 ps for P3HT:bisPCBM (see Table 1), which are both considerably shorter as compared to the thermally annealed films. It is important to note that the measured difference is larger than the instrumental resolution that is ~3 ps in these experimental conditions.

The correlation of these results with the device performance indicates that the microstructure of the bulk heterojunction plays a fundamental role. As mentioned above, the lifetime of the photoexcitations in the blends is determined both by the exciton diffusion (dominated by the microstructure of the film) and by the electron transfer process. To eliminate the effect of the exciton diffusion and microstructure of the film, we also performed time-resolved PL measurements of both blends in solution. We assume that in solution the distribution of the polymer and of the fullerene derivatives is homogeneous, allowing us to investigate the influence of the LUMO level variation on the PL dynamics. To promote the interaction between the polymer and the fullerene molecules, the measurements were performed in relatively concentrated solutions (10 mg/mL). Figure 4(a) reports the PL spectra of P3HT, P3HT:PCBM, and P3HT:bisPCBM in solution. The spectral shape for the three samples is the same, with the maximum intensity

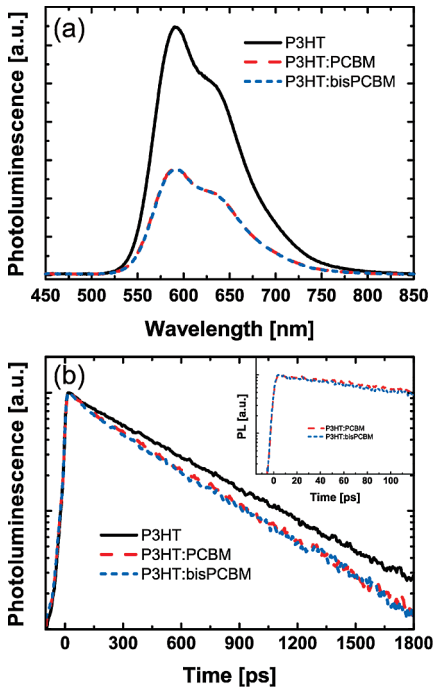

Figure 4. (a) Photoluminescence spectra and (b) dynamics detected at ~590 nm of P3HT, P3HT:PCBM, and P3HT:bisPCBM in ODCB solution. The inset shows the dynamics in the shorter time range.

centered at ~590 nm and a shoulder at ~630 nm. Upon blending with the two fullerene derivatives, the PL of the polymer is quenched by a factor 2.3. Figure 4(b) shows the PL dynamics for P3HT, P3HT:PCBM, and P3HT:bisPCBM in solution, integrated over the wavelength range corresponding with the PL maximum (~590 nm). The PL lifetime of P3HT was fitted with two time constants τ_1 ~172 and τ_2 ~510 ps. Both cosolutions exhibit faster dynamics with respect to the neat P3HT with time constants τ_1 ~71 and τ_2 ~413 ps, indicating the occurrence of the electron transfer process. Moreover, we can assume safely that the average distance between a polymer chain and an acceptor molecule in the cosolutions with the two different acceptors is similar. The inset of Figure 4 shows the PL dynamics of both donor/acceptor cosolutions, detected in a short time range with resolution ~3 ps. Also, in this case the dynamics for the PCBM- and bisPCBM-based solutions are identical. This result shows that the different dynamics in the thermally annealed and slowly dried thin films for the blends with the two acceptors are determined by the microstructure of the films. When the polymer domains are large compared to the exciton diffusion length, the electron transfer will be limited, resulting in a longer PL lifetime. Although both the PCBM- and bisPCBM-based thin film blends were prepared with the same procedure, the crystallization process can be rather different for the two fullerene derivatives. The formation of thin films from solution is not only determined by the processing conditions but also by the chemical structure of the components.[22] A variation of the solubility of the compounds and of their compatibility can have an enormous effect on the thermodynamics of the film formation.

To further investigate the differences in the microstructure of the two blends, tapping mode atomic force microscopy (AFM) was used. Figure 5 shows the height images of the spin-coated and subsequently annealed films as well as the slowly dried thin films of P3HT:PCBM (Figure 5 (a),(c)) and P3HT:bisPCBM (Figure 5(b),(d)). For films prepared by thermal annealing, the surfaces are smoother with a root-mean-square

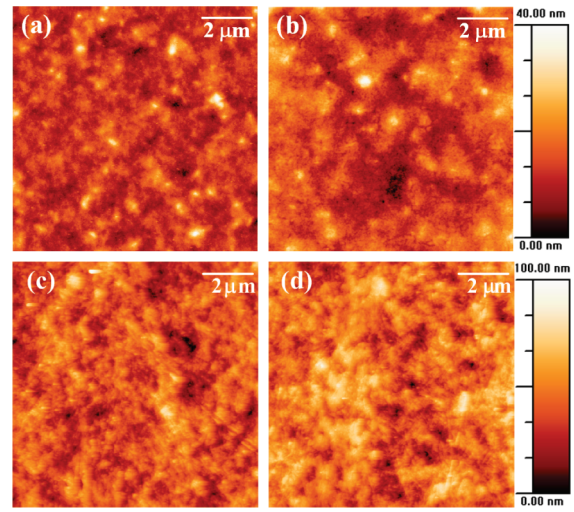

Figure 5. TM-AFM height images of P3HT:PCBM (a), P3HT:bisPCBM (b), thermal annealed films and P3HT:PCBM (c), P3HT:bisPCBM, and (d) slowly dried films.

(rms) roughness of ~3.9 and ~4.6 nm for P3HT:PCBM and P3HT:bisPCBM, respectively. The slowly dried films exhibit rms roughness of ~10.7 nm for P3HT:PCBM and ~12.4 nm for P3HT:bisPCBM. Besides the difference in roughness between the blends prepared with different processing conditions, the blends prepared with PCBM are slightly smoother than the ones with bisPCBM in both processing conditions. Moreover, the AFM phase contrast images do not show evidence of phase segregation.

While AFM gives information only about the surfaces, as already mentioned, information about the three-dimensional structure of the blends can be extracted from the dynamics of the photoluminescence. The average domain size in the bulk heterojunction can be estimated to be equivalent to the average diffusion distance of the excitons $d = \sqrt{\tau D}$, where τ is the PL decay time and D is the exciton diffusion coefficient. The exciton diffusion coefficient can be extracted by using the exciton diffusion length $L_P = 5.3$ nm reported in the literature for thermally annealed P3HT thin films[6] and the PL decay time measured for our samples. In this way, we obtained that the average size of the domains in thermally annealed P3HT:PCBM is 16% smaller than the average size of the domains of P3HT:bisPCBM films. In the case of slowly dried samples, the estimation is more difficult because a precise value of the diffusion length, which might be different with respect to the thermally annealed layers due to the increased crystallinity, is not available. If we assume, however, a similar diffusion length as in the thermally annealed film, we obtain that the P3HT domains in the PCBM-based blend are 10% smaller than in the bisPCBM-based one. All these observations suggest a nonoptimal three-dimensional morphology.

The fact that the microstructure of the P3HT:bisPCBM solar cells is not yet optimized is also reflected in a comparison of the device performance with P3HT:PCBM cells. The slightly lower external quantum efficiency as well as the lower short-circuit current density in P3HT:bisPCBM devices compared to P3HT:PCBM cells also point to a nonideal microscopic structure of the bulk heterojunction. Our results demonstrate that a further enhancement of the performance of P3HT:bisPCBM solar cell performances is possible by optimization of the bulk herero-junction microscopic structure.

3. Conclusion

We have studied the dynamics of the photoexcitations in blends of P3HT and bisPCBM, a new acceptor material with its LUMO level 100 meV higher than PCBM. By comparison with the standard PCBM blend, we obtain insight into the efficiency and dynamics of the charge generation in P3HT:bisPCBM. Thin films prepared using different protocols were studied to discern between the effect of the microstructure of the solid state arrangement and the variation of the LUMO offset on the charge transfer dynamics. In solution, the two blends exhibit the same dynamics of the photoluminescence, showing that the variation of the energy level offset, which increases the V_{oc} in solar cells devices, does not play a detrimental role in the efficiency of the exciton dissociation. In thin films, however, prepared by thermal annealing and slow drying, P3HT:bisPCBM shows a slower dynamics than P3HT:PCBM. Since the dynamics of the PL are governed by a combination of exciton diffusion and exciton dissociation, these measurements not only provide information on the electron transfer process but also on the microstructure of the bulk heterojunction. The slower dynamics in the P3HT:bisPCBM is ascribed to radiative losses caused by a nonoptimal three-dimensional structure of the bulk heterojunction in the slow dried films. This finding indicates that there is a close correlation between the performance of the devices, the three-dimensional structure, and the dynamics of the photoexcitations in the blend.

4. Experimental Section

Sample Fabrication. Thin films of P3HT:PCBM and P3HT:bisPCBM were prepared with two different techniques: thermal annealing and slow drying. The weight ratio between the blend components was: 1:1 for P3HT:PCBM and 1:1.2 for P3HT:bisPCBM, to compensate the molecular weight difference between the two acceptors. The thin films were spin coated from 20 mg/mL of solution in solvent. For the measurements in solution, ODCB (*ortho*-dichlorobenzene) was used as solvent.

Thermal Annealing Technique. The thin films were processed from chloroform, and after spin coating the samples were annealed at 135 °C for 15 min. The thin films prepared by thermal annealing have a thickness ∼350 nm.

Slow Drying Technique. The thin films were processed from ODCB, and after spin coating the samples were left to dry in a closed Petri dish for 48 h. After the solvent annealing, they were thermally annealed for 5 min at 110 °C. The thin films prepared by thermal annealing have a thickness ∼150 nm.

Prior to processing, the substrates were cleaned with a standard wet-cleaning procedure, combining ultrasonic cleaning in acetone and isopropanol.

Spectroscopy. PL emission was induced by the second harmonic of a Ti:sapphire laser delivering pulses of 150 fs width at 380 nm. The signal was recorded by a Hamamatsu streak camera functioning in synchroscan with ∼2 ps time resolution. All time-resolved measurements were carried out at room temperature. The thin films were placed in an optical cryostat at $\sim 10^{-5}$ mbar to prevent photo-oxidation. Solutions were placed in 2 mm quartz cuvettes. The PL measurements on thin films were performed in transmission mode and on solutions in reflection mode. The PL spectra were corrected for the spectral response of the setup. The overlap of the PL spectra and absorption spectra for bulk heterojunction is negligible, and therefore the PL spectra were not corrected for self-absorption. The traces of the PL decay time were integrated at the 0−0 excitonic transition in the spectral region of about 20 nm. The PL decay detected at 0−1 excitonic transition (not shown in the paper) presents the same trend as the one at the 0−0 transition. The measurements were performed for different series of samples prepared by following the same fabricating protocols. The results show high reproducibility for different samples and sample position. The variations in the results of the PL measurements do not exceed the resolution of the instrument.

Surface Topography Measurements. AFM images were taken on a MultiMode AFM with NanoScope IV Scanning Probe Microscope Controller.

References and Notes

(1) Yu, G.; Gao, J.; Hummelen, J.; Wudl, F.; Heeger, A. *Science* **1995**, *270*, 1789–1791.
(2) Yu, G.; Heeger, A. J. *J. Appl. Phys.* **1995**, *78*, 4510–4515.
(3) Koch, N. *ChemPhysChem* **2007**, *8*, 1438–1455.
(4) Campoy-Quiles, M.; Ferenczi, T.; Agostinelli, T.; Etchegoin, P. G.; Kim, Y.; Anthopoulos, T. D.; Stavrinou, P. N.; Bradley, D. D. C.; Nelson, J. *Nat. Mater.* **2008**, *7*, 158–164.
(5) Shaheen, S. E.; Brabec, C. J.; Sariciftci, N. S.; Padinger, F.; Fromherz, T.; Hummelen, J. C. *Appl. Phys. Lett.* **2001**, *78*, 841–843.
(6) Kroeze, J. E.; Savenije, T. J.; Vermeulen, M. J. W.; Warman, J. M. *J. Phys. Chem. B* **2003**, *107*, 7696–7705.
(7) Mikhnenko, O. V.; Cordella, F.; Sieval, A. B.; Hummelen, J. C.; Blom, P. W. M.; Loi, M. A. *J. Phys. Chem. B* **2008**, *112*, 11601–11604.
(8) Muhlbacher, D.; Scharber, M.; Morana, M.; Zhu, Z.; Waller, D.; Gaudiana, R.; Brabec, C. *Adv. Mater.* **2006**, *18*, 2884–2889.
(9) Kim, Y.; Cook, S.; Tuladhar, S. M.; Choulis, S. A.; Nelson, J.; Durrant, J. R.; Bradley, D. D. C.; Giles, M.; McCulloch, I.; Ha, C.; Ree, M. *Nat. Mater.* **2006**, *5*, 197–203.
(10) Lenes, M.; Wetzelaer, G. A. H.; Kooistra, F. B.; Veenstra, S. C.; Hummelen, J. C.; Blom, P. W. M. *Adv. Mater.* **2008**, *20*, 2116–2119.
(11) Brabec, C. J.; Cravino, A.; Meissner, D.; Sariciftci, N. S.; Fromherz, T.; Rispens, M. T.; Sanchez, L.; Hummelen, J. C. *Adv. Funct. Mater.* **2001**, *11*, 374–380.
(12) Koster, L. J. A.; Mihailetchi, V. D.; Blom, P. W. M. *Appl. Phys. Lett.* **2006**, *88*, 093511−3.
(13) Li, G.; Shrotriya, V.; Huang, J.; Yao, Y.; Moriarty, T.; Emery, K.; Yang, Y. *Nat. Mater.* **2005**, *4*, 864–868.
(14) Halls, J. J. M.; Cornil, J.; dos Santos, D. A.; Silbey, R.; Hwang, D.; Holmes, A. B.; Bredas, J. L.; Friend, R. H. *Phys. Rev. B* **1999**, *60*, 5721.
(15) Yu, J.; Hu, D.; Barbara, P. F. *Science* **2000**, *289*, 1327–1330.
(16) Mihailetchi, V.; Xie, H.; de Boer, B.; Popescu, L.; Hummelen, J.; Blom, P.; Koster, L. *Appl. Phys. Lett.* **2006**, *89*.
(17) Mihailetchi, V.; Duren, J. V.; Blom, P.; Hummelen, J.; Janssen, R.; Kroon, J.; Rispens, M.; Verhees, W.; Wienk, M. *Adv. Funct. Mater.* **2003**, *13*, 43–46.
(18) Yang, X.; Loos, J.; Veenstra, S.; Verhees, W.; Wienk, M.; Kroon, J.; Michels, M.; Janssen, R. *Nano Lett.* **2005**, *5*, 579–583.
(19) Sundberg, M.; Inganas, O.; Stafstrom, S.; Gustafsson, G.; Sjogren, B. *Solid State Commun.* **1989**, *71*, 435–439.
(20) Li, G.; Yao, Y.; Yang, H.; Shrotriya, V.; Yang, G.; Yang, Y. *Adv. Funct. Mater.* **2007**, *17*, 1636–1644.
(21) Österbacka, R.; An, C. P.; Jiang, X. M.; Vardeny, Z. V. *Science* **2000**, *287*, 839–842.
(22) Katz, H. E.; Bao, Z. *J. Phys. Chem. B* **2000**, *104*, 671–678.

JP907840Z